

## Optimization of fuzzy photovoltaic maximum power point tracking controller using chimp algorithm

Ammar Al-Gizi, Abbas Hussien Miry, Mohanad A. Shehab

Department of Electrical Engineering, College of Engineering, Mustansiriyah University, Baghdad, Iraq

### Article Info

#### Article history:

Received Jul 21, 2021

Revised May 20, 2022

Accepted Jun 5, 2022

#### Keywords:

Chimp algorithm

Fuzzy logic controller

Maximum power point tracking

Optimization

Photovoltaic

### ABSTRACT

In this paper, a photovoltaic (PV) fuzzy maximum power point tracking (MPPT) method optimized by the chimp algorithm is presented. The fuzzy logic controller (FLC) of seven triangular membership functions (MFs) is used. The optimization fitness function is composed of transient and steady-state indices under different irradiation and temperature operating conditions. By using MATLAB package, the performance of optimized method is examined and compared with asymmetrical FLC and well-known perturb and observe (P&O) tracking methods at different operating conditions in terms of: transient rising time ( $t_r$ ) and energy yield during 30 s. Moreover, the tracking methods are also compared in terms of the fitness function value. From the comparison of simulation results, a more energy can be harvested by using the proposed optimized tracking method compared to the other methods. Consequently, at the various operating conditions, the proposed method can be used as a more reliable tracking method for PV systems.

*This is an open access article under the [CC BY-SA](https://creativecommons.org/licenses/by-sa/4.0/) license.*



### Corresponding Author:

Ammar Al-Gizi

Department of Electrical Engineering, College of Engineering, Mustansiriyah University

Bab Al Muadham, 10047, Baghdad, Iraq

Email: ammar.ghalib@uomustansiriyah.edu.iq

## 1. INTRODUCTION

The speed and accuracy of maximum power point tracking (MPPT) represent important performances in photovoltaic (PV) systems to increase the harvested energy yield under different operating conditions [1]. For this purpose, many of classical and intelligent MPPT methods are recommended in the literature [2]–[10]. The shape and number of membership functions (MFs) used in the fuzzy MPPT affect the tracking performances. Meanwhile, the fuzzy MPPT method of seven triangular-shaped MFs can provide the best transient and steady tracking performances [11].

The fuzzy logic controller (FLC) can be further optimized to improve the tracking performances by tuning the values of MFs' parameters using individual or combination of different intelligent techniques as genetic algorithm (GA), particle swarm optimization (PSO), and artificial neural networks (ANN) [12]–[18]. In this work, an asymmetrical FLC tracking method of seven triangular-shaped MFs is used, where its MFs' values are derived based on power-voltage (P-V) characteristics under standard technical conditions (STC) of irradiation  $1000 \text{ W/m}^2$  and cell temperature  $25 \text{ }^\circ\text{C}$ . Moreover, the MFs of fuzzy MPPT method is optimized using the chimp optimization algorithm. In the optimization process, the fitness function is a weighted sum of a cost function under different irradiation and temperature operating conditions. Where, the cost function is composed of transient and steady state indices at each operating condition. The tracking performances of the optimized fuzzy tracking method are examined and compared with the asymmetrical and classical well-known perturb and observe (P&O) tracking methods in terms of rising time ( $t_r$ ) and energy yield from the PV module, and the fitness function value.

## 2. PHOTOVOLTAIC (PV) SYSTEM MODELING

In this work, a BPSX150S PV module of 72 series solar cells is used. Under STC, this module has a maximum power point (MPP) of maximum power of 150 W at module voltage and current of 34.5 V and 4.35 A, respectively [19]. Since the location of MPP is changed by changing irradiation ( $G$ ) and temperature ( $T$ ) conditions, the extracted power and energy yield from PV are subsequently changed. Consequentially, using a proper tracking method to maintain the MPP is an essential role to improve the PV system performance. Figure 1 depicts the PV system including a fuzzy MPPT controller used in this work.

For a single-diode model, the operating point current of PV module at different module voltage ( $V$ ), irradiation ( $G$ ), and cell temperature ( $T$ ) can be represented by [20], [21]:

$$I = f(V, G, T) = I_{ph} - I_o \left( \exp \left( \frac{q(V+IR_s)}{N_s nKT} \right) - 1 \right) - \left( \frac{V+IR_s}{R_{sh}} \right), \tag{1}$$

where  $I_{ph}$  is the photocurrent or short-circuit current ( $I_{sc}$ ).  $R_s$  and  $R_{sh}$  are the series and parallel resistances of the PV cell, respectively.  $q$  is the electron charge ( $1.602 \times 10^{-19}$  C),  $K$  is the Boltzmann's constant ( $1.381 \times 10^{-23}$  J/K),  $n$  is the diode ideality factor (1.62 in this work),  $N_s$  is the number of series solar cells constructing the PV module (72 in this work).  $I_o$  is the diode's reverse saturation current which is affected by the cell temperature.  $I_o$  equation can be described by (2):

$$I_o = I_{or} \times \left( \frac{T}{T_r} \right)^3 \times \exp \left( \frac{qE_g}{nK} \left( \frac{1}{T_r} - \frac{1}{T} \right) \right), \tag{2}$$

where  $T_r$  is the temperature at STC which is 298 °K or 25 °C.  $E_g$  is the band-gap energy of the semiconductor used in cell manufacturing.  $I_{sc}$  which is influenced by  $T$  and  $G$  is presented as (3):

$$I_{sc} = \frac{G}{G_r} (I_{scr} + \alpha(T - T_r)), \tag{3}$$

where  $G_r$  is the irradiation at STC and  $\alpha$  is the coefficient of short circuit current temperature [20], [21].

Figure 2 shows the ( $I$ - $V$  and  $P$ - $V$ ) and the corresponding  $\Delta P/\Delta V$  characteristics of the PV module at various  $G$  and constant  $T$  of 25 °C. Where Figure 2(a) shows the  $I$ - $V$  and  $P$ - $V$  characteristics while Figure 2(b) shows the corresponding  $\Delta P/\Delta V$  characteristics (absolute value). It is obvious from Figure 2(b) that the  $\Delta P/\Delta V$  is smoothly changed. Hence, it is used as a suitable input of the fuzzy MPPT controller.

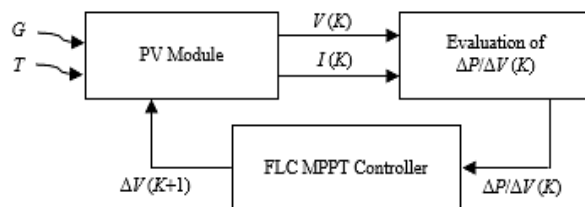


Figure 1. PV system including fuzzy MPPT controller

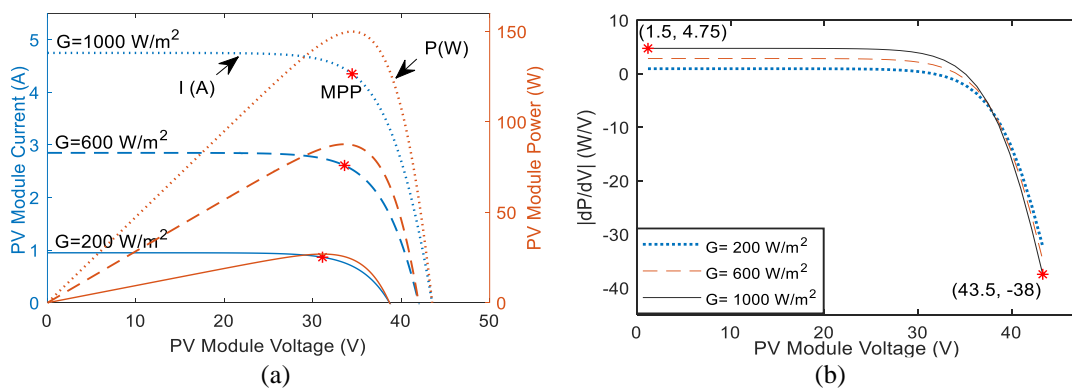


Figure 2. At various  $G$  and constant  $T=25$  °C: (a)  $I$ - $V$  and  $P$ - $V$  characteristics and (b)  $|dP/dV|$  characteristics

### 3. ASYMMETRICAL FUZZY MPPT CONTROLLER

The Fuzzy MPPT method has promising results compared with classical tracking methods as P&O, InC [22], [23]. Hence, in this paper, it is used to track and maintain the MPP by continuing updating the PV module voltage by suitable PV voltage change ( $\Delta V$ ). Accordingly, the FLC input is the PV power-voltage slope ( $\Delta P/\Delta V$ ) while the output is  $\Delta V$ . FLC can be classified into different types according to the definition of setting values, shapes, and number of the used membership functions (MFs). In this paper, an asymmetrical FLC of seven triangular-shaped MFs is used due to its superior results compared with five bell and triangular MFs [11], [20]. The asymmetrical MFs of the input  $\Delta P/\Delta V$  is shown in Figure 3. Where symbols NB, NM, NS, Z represents negative big, negative medium, negative small, and zero, respectively. Whereas, PB, PM, PS represents positive big, positive medium, and positive small, respectively.  $x_1, x_2, x_3, x_4, x_5$  and  $x_6$  are setting values of asymmetrical input's MFs. These values are determined based on the design strategy developed in [11].

Under STC, the minimum and maximum values of  $\Delta P/\Delta V$  are  $-38 \text{ W/V}$  and  $4.75 \text{ W/V}$ , respectively as shown in Figure 2(b). Hence, the maximum negative value of  $\Delta P/\Delta V$  ( $x_1$  in Figure 3) is  $-38$ , whereas the maximum positive value of  $\Delta P/\Delta V$  ( $x_6$  in Figure 3) is  $4.75$ . Consequently, the six setting values of MFs are  $x_1=-38, x_2=-25.33, x_3=-12.67, x_4=1.58, x_5=3.16,$  and  $x_6=4.75$ . In contrast, seven MFs of the output  $\Delta V$  are shown in Figure 4, where the chosen minimum and maximum setting values are  $-1.5$  and  $1.5$ , respectively. The FLC rules can be easily concluded from observing Figure 2(b). Since the output  $\Delta V$  is linearly depend on the input  $\Delta P/\Delta V$ . Subsequently, the seven rules depicted in Table 1 are used [11]. Furthermore, in this paper, an optimization method is proposed to optimize the setting values of the asymmetrical FLC MPPT method for improving the PV tracking performance. The next section describes the proposed tracking method.

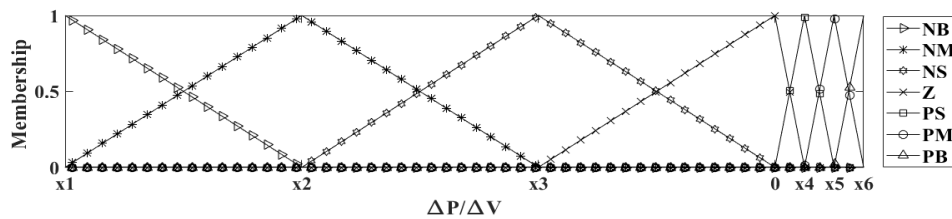


Figure 3. MFs of asymmetrical FLC input  $\Delta P/\Delta V$

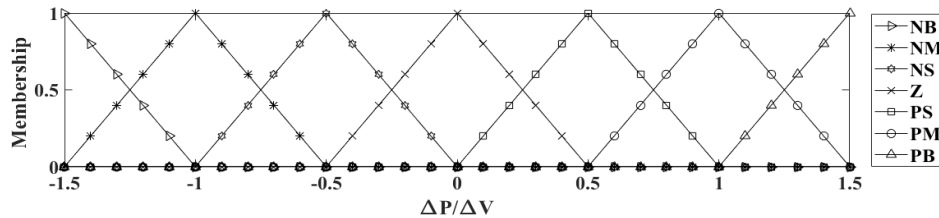


Figure 4. MFs of asymmetrical FLC output  $\Delta V$

Table 1. The rules of FLC

$\Delta P/\Delta V$	NB	NM	NS	Z	PS	PM	PB
$\Delta V$	NB	NM	NS	Z	PS	PM	PB

### 4. OPTIMIZED FLC USING CHIMP ALGORITHM

The optimization of MFs' setting values plays an essential role in improving the tracking performance. For this purpose, many algorithms can be used [15]-[18]. In this paper, the chimp algorithm is used to optimize the six setting values of FLC input  $\Delta P/\Delta V$ . In the following sub-sections, the chimp optimization algorithm and its details for optimizing the MFs' setting values are presented.

#### 4.1. Chimp optimization algorithm

The chimps' society is based on fission and fusion. The mixture of society in this type of society varies over time. Furthermore, each member of society has a unique capacity and a distinct responsibility, all of which may alter over time. With this in mind, this algorithm proposes the idea of separate groups, in which

each chimps' group attempts to learn about the search area using its unique capacity for a specific task. There are four types of the chimps were given the names of “driver”, “barrier”, “chaser”, and “attackers”. They have a variety of responsibilities in the hunting process to ensure a good hunt. The preys are pursued by the drivers, who do not try to catch them. Barriers erect themselves in trees to build a dam across the prey's escape route. Chasers run quickly after their preys in order to catch them. Finally, the attackers anticipate the prey's descent into the lower canopy. Attackers must be more intelligent in anticipating the prey's next movements. As a result, after a good search, Attackers get a bigger piece of meat as a reward. This important task (attacking) is linked to age, intelligence, and physical capacity. Furthermore, chimps may switch roles during a hunt or remain in the same role during the process [24]. To summarize, chimps' social hunting There are two parts to this activity: "exploration" which comprises moving, Defending and pursuing the prey, and "exploitation", it requires going after the prey. Figure 5 depicts the two stages. Where Figures 5(a) and 5(b) depict the exploration and exploitation stages, respectively.

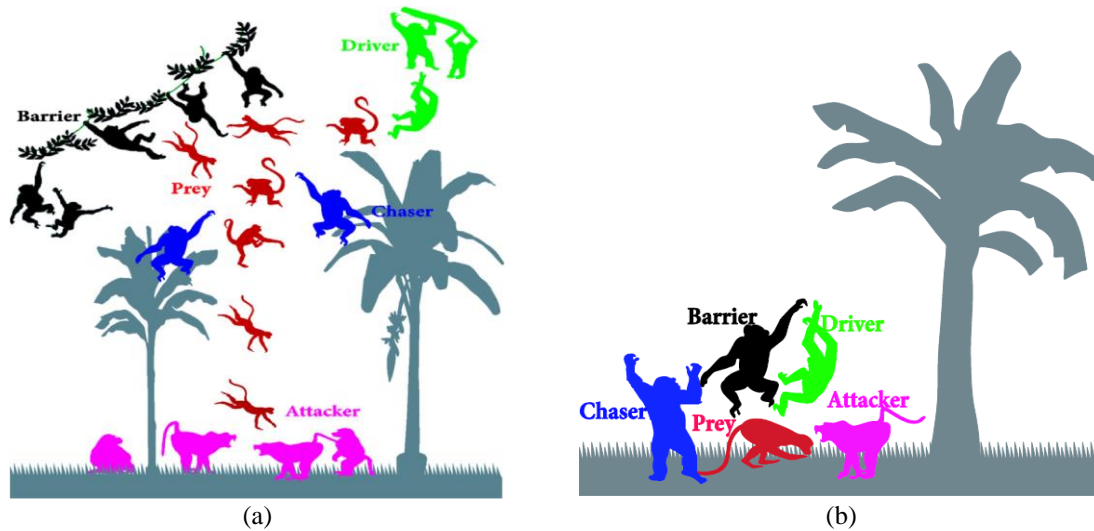


Figure 5. The major stages of chimp's operations: (a) exploration and (b) exploitation

#### 4.1.1. Driving and chasing the prey

The prey is hunted during the exploration and extraction processes, as previously mentioned. As shown in (4) and (5) are used to model driving and chasing the prey mathematically [24]:

$$x_{chimp}(n+1) = x_{prey}(n) - a \cdot d, \quad a = 2 \cdot f_1 \cdot Rd_1 - a \quad (4)$$

$$d = |c \cdot x_{prey}(n) - m \cdot x_{chimp}(n)|, \quad c = 2 \cdot Rd_2 \quad (5)$$

where  $n$  represents the current iteration,  $m$  is chaotic value,  $x_{chimp}(n)$  and  $x_{prey}(n)$  are the chimp and prey position vectors, respectively.  $Rd_1$  and  $Rd_2$  are the random values with the values of  $[0,1]$ . Through the iteration,  $f$  is nonlinearly decreased from 2.5 to 0.

#### 4.1.2. Exploration stage

Two methods are designed to mathematically model chimp attacking behavior: at first, the chimps investigate the prey's position using driving, obstructing and pursuing, then they might be able to encircle it. Finally, attackers are normally in charge of the hunt. The search sometimes includes driver, barrier, and chaser [24].

$$\begin{aligned} d_{attack} &= |c_1 x_{attack} - m_1 d|, \quad d_{barrier} = |c_2 x_{barrier} - m_2 x|, \\ d_{chaser} &= |c_3 x_{chaser} - m_3 x|, \quad d_{driver} = |c_4 x_{driver} - m_4 x| \\ x_1 &= x_{attack} - a_1 d_{attack}, \quad x_2 = x_{barrier} - a_2 d_{barrier} \end{aligned} \quad (6)$$

$$x_3 = x_{chaser} - a_3 d_{chaser}, x_2 = x_{driver} - a_4 d_{driver}, \tag{7}$$

$$x(n) = \frac{x_1 + x_2 + x_3 + x_4}{4} \tag{8}$$

As shown in Figure 6, the chimp's location in space of the search is modified in relation to the positions of other chimps. As shown, the final location of the chimp is determined at random inside a circle. Where a circle is identified by the positions of the attacker, barrier, chaser, and drivers.

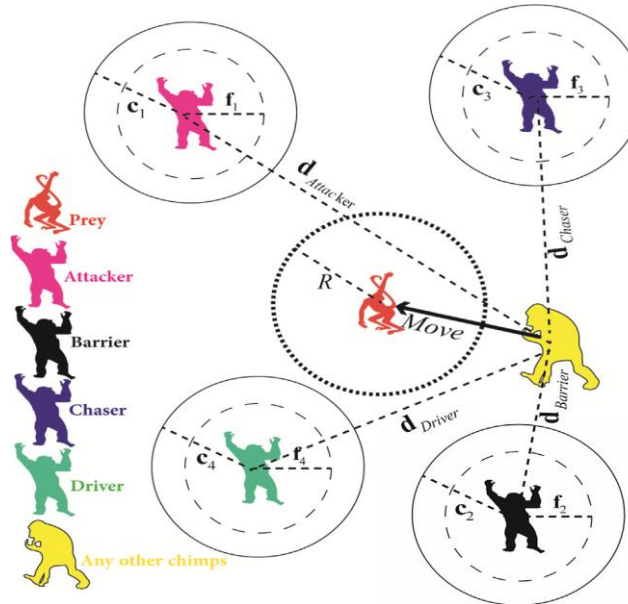


Figure 6. Position update position

**4.1.3. Exploitation stage**

The chimps split up to look for prey and then they all come together to attack it. This action is formally modelled using the vector *a*, as shown in Figure 7. Where, the condition  $1 < |a|$  causes chimps to deviate from prey to avoiding entrapment in local optimal point and condition  $1 > |a|$  causes chimps to confluence at the prey site to get global optimal point.

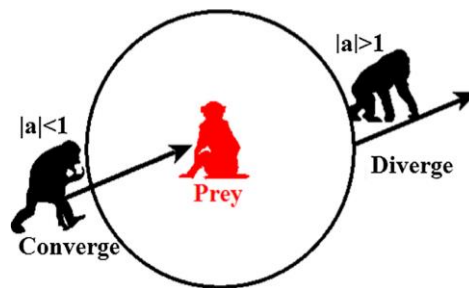


Figure 7. The parameter “a” effecting on the updating operation

**4.1.4. Improved the exploitation stage**

As previously mentioned, the social reward in chimp society is based on hunting meat. In the final phase, chimps are forced to give up their hunt behavior by attempting to steal the meat. Own hunting responsibilities as a result, they attempt in a haphazard manner to steal hunting meat for social purposes. Chaotic maps can be used to model the chimps' chaotic behavior in the final stage. The updating operation can be modeled as [24]:

$$x_{chimp}(n+1) = \begin{cases} x_{prey}(n) - a * d & \text{if } \mu < 0.5 \\ \text{Chaotic value} & \text{if } \mu \geq 0.5 \end{cases} \quad (9)$$

where  $\mu$  is a value between zero and one.

#### 4.2. Optimization of MFs' setting values using chimp algorithm

The chimp algorithm is used to optimize the MFs' setting values of FLC input  $\Delta P/\Delta V$ :  $x_1$ ,  $x_2$ ,  $x_3$ ,  $x_4$ ,  $x_5$ , and  $x_6$  by optimizing the intervals between setting values:  $xx_1$ ,  $xx_2$ ,  $xx_3$ ,  $xx_4$ ,  $xx_5$ , and  $xx_6$ . Meanwhile, the optimization process can be defined by maximizing the fitness function  $f$  ( $xx_1$ ,  $xx_2$ ,  $xx_3$ ,  $xx_4$ ,  $xx_5$ , and  $xx_6$ ). Where  $x(1)=-xx(1)-xx(2)-xx(3)$ ,  $x(2)=-xx(1)-xx(2)$ ,  $x(3)=-xx(1)$ ,  $x(4)=xx(4)$ ,  $x(5)=xx(4)+xx(5)$ ,  $x(6)=xx(4)+xx(5)+xx(6)$ , based on the constraints:

$$0 < xx_1 + xx_2 + xx_3 < NEG_{max},$$

$$0 < xx_4 + xx_5 + xx_6 < POS_{max},$$

where the selected values of  $NEG_{max}$  and  $POS_{max}$  in this work are 50 and 10, respectively.

The goal of optimization is maximizing the energy yield from the PV module and minimization the rising time at different irradiation and temperature operating conditions. Subsequently, in this paper, the chosen fitness function "Fitness" is a weighted sum of a cost function at five different operating conditions of  $G$  and  $T$  (in Iraq). Hence, the fitness function can be defined as (10):

$$Fitness = \sum_{i=1}^5 Cost(i) w(i) \quad (10)$$

where  $Cost(i)$  is the cost function which is composed of transient and steady-state response indices at the operating condition  $i$  as (11):

$$Cost(i) = \left[ 0.3 \left( \frac{t_f - t_r}{t_f} \right) + 0.7 \frac{\int_{t_r}^{t_f} V(t)I(t)dt}{\int_{t_r}^{t_f} P_{MPP}dt} \right] \times 100\% \quad (11)$$

where  $t_f$  is final time of simulation [11]. Whereas,  $w(i)$  is the weight of the operating condition  $i$ . The best fitness function value is 1.

In this work, the chosen values of weights are 0.25, 0.166, 0.084, 0.33, and 0.17 corresponding to the five chosen operating conditions (in Iraq) defined by  $G(i)$  of 400 W/m<sup>2</sup>, 600 W/m<sup>2</sup>, 1000 W/m<sup>2</sup>, 800 W/m<sup>2</sup>, 1000 W/m<sup>2</sup>, and  $T(i)$  of 25 °C, 35 °C, 25 °C, 45 °C, and 45 °C, respectively. According to each set of setting values, the fuzzy MPPT is simulated at five different operating conditions to calculate the corresponding fitness function value. Finally, the best solution is chosen.

## 5. RESULTS AND DISCUSSION

During the optimization and test phases, the chosen initial operating PV voltage is 1 V (at left of MPP). The performance of the optimized tracking method is examined by MATLAB simulation for 30 s at different operating conditions. Furthermore, results of the proposed method are compared with the classical P&O method and asymmetrical FLC method (explained in section 3) in terms of rising time ( $t_r$ ) and energy yield from the PV module. Where the energy yield in (Wh) can be expressed by [7].

$$Energy\ yield = \frac{\int_0^{t_f} V(t)I(t)dt}{3600} \quad (12)$$

According to the optimized FLC by chimp algorithm, the optimized solution is  $xx_1=5.3364$ ,  $xx_2=4.8655$ ,  $xx_3=6.4194$ ,  $xx_4=0.0048$ ,  $xx_5=0.9542$ , and  $xx_6=0.9398$ . Consequently, the MFs' setting values of  $\Delta P/\Delta V$  are  $x_1=-16.6213$ ,  $x_2=-10.2019$ ,  $x_3=-5.3364$ ,  $x_4=0.0048$ ,  $x_5=0.959$ , and  $x_6=1.8988$ . Hence, Figure 8 is shown the corresponding MFs of asymmetrical and optimized FLC tracking methods are shown in Figures 8(a) and 8(b), respectively.

Figure 9 is shown at STC and by using the different tracking methods, Figures 9(a) and 9(b) show the PV power and energy yield, respectively. Where maximum output power and energy can be harvested from the used PV module under this condition are 149.9873 W and 1.2499 Wh, respectively. In the same context, Table 2 illustrates the comparative results of the tracking methods under STC. In contrast, Figure 10

shows the power as shown in Figure 10(a) and energy yield in Figure 10(b) curves, respectively at operating condition of  $G=400 \text{ W/m}^2$  and  $T=25 \text{ }^\circ\text{C}$ . Where the maximum output power and energy can be harvested from the module under this condition are 56.8948 W and 0.4741 Wh, respectively. Whereas, the comparative results of the tracking methods under this operating condition are illustrated in Table 3. Since the MFs' setting values of asymmetrical FLC method is derived under STC, hence its tracking performances are obviously close to the tracking results of optimized method at STC as shown in Figure 9 and Table 2. Whereas the asymmetrical FLC method failed to satisfy the optimal results under the other operating condition of  $G=400 \text{ W/m}^2$  and  $T=25 \text{ }^\circ\text{C}$  as shown in Figure 10 and Table 3.

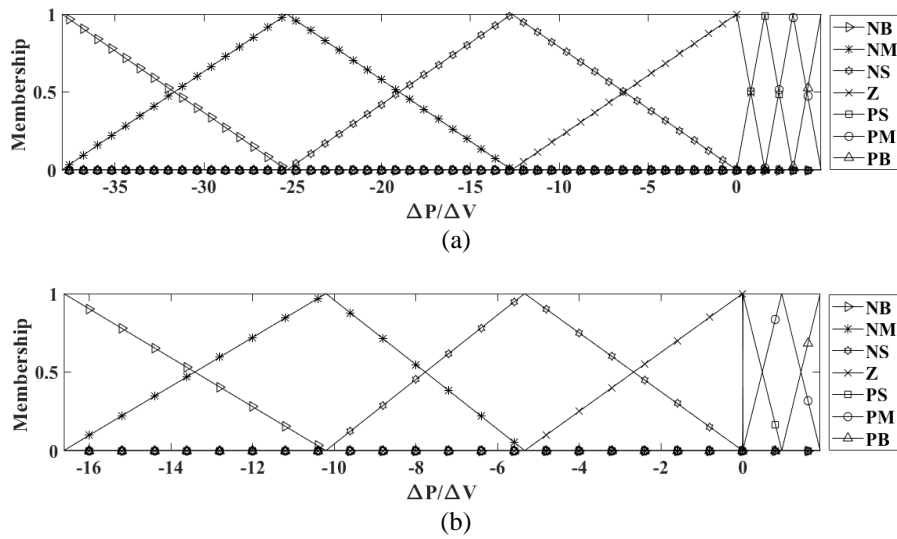


Figure 8. MFs of  $\Delta P/\Delta V$ : (a) asymmetrical FLC MPPT and (b) optimized FLC MPPT

In contrast, the optimized tracking method can successfully track the MPP with less rising time compared with asymmetrical method. Consequently, a more energy is harvested under different conditions as shown in Figures 9 and 10. Where in the case of  $G=400 \text{ W/m}^2$  and  $T=25 \text{ }^\circ\text{C}$ , energy of 0.4581 Wh with rising time of 2 s are harvested by using the optimized method, in contrast, energy of 0.4386 Wh, 0.4515 Wh, and 0.4299 Wh with rising times of 4.4 s, 0.8 s, 5.3 s are harvested using asymmetrical, P&O (at  $\Delta V=3.5 \text{ V}$ ), and P&O (at  $\Delta V=0.5 \text{ V}$ ) tracking methods, respectively.

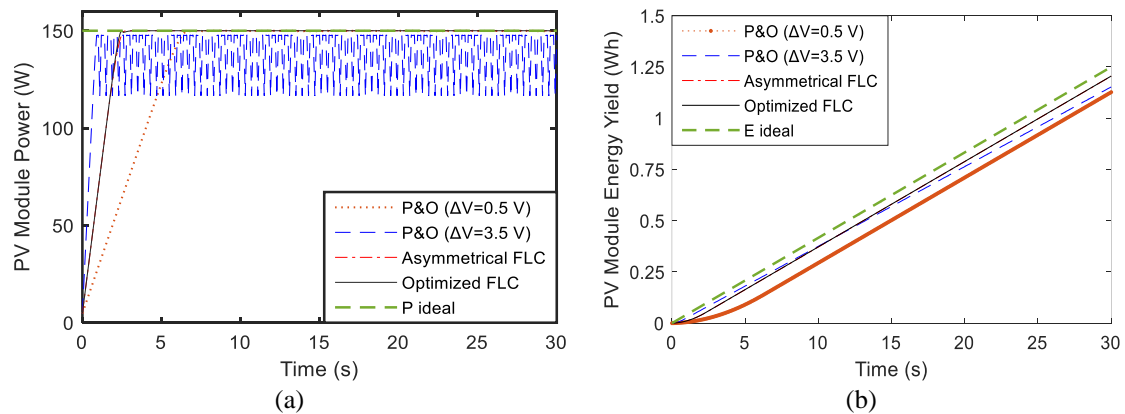
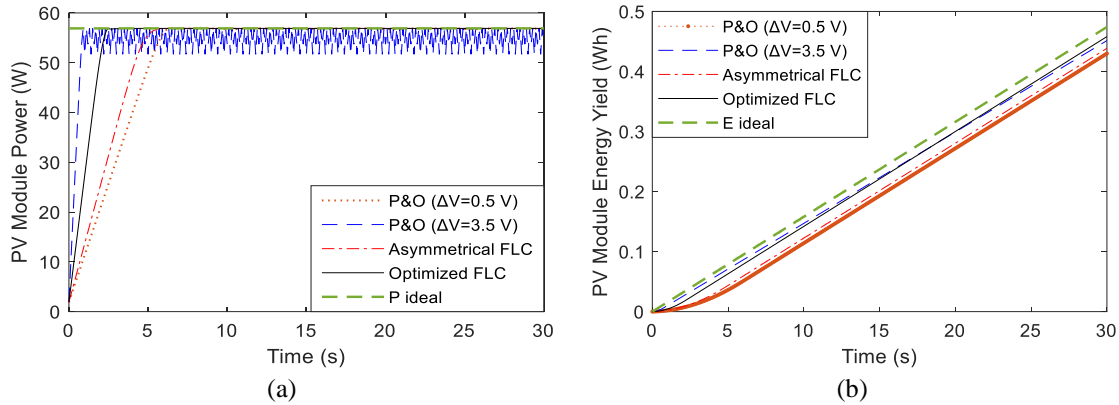


Figure 9. PV power and energy yield under STC: (a) power and (b) energy yield

Moreover, the performance of the optimized method is compared with the other tracking methods in terms of fitness function value. Table 4 depicts the comparison results. In future the system can be improved using different objective function as in [25]–[27].

Table 2. Comparative results of tracking methods under STC

Tracking Method	Rising Time (s)	Energy Yield (Wh)
P&O (at $\Delta V=0.5$ V)	5.6	1.1269
P&O (at $\Delta V=3.5$ V)	0.8	1.1525
Asymmetrical FLC	2.2	1.2051
Optimized FLC by chimp algorithm	2.1	1.2055

Figure 10. PV power and energy yield at  $G=400$  W/m<sup>2</sup> and  $T= 25$  °C: (a) power and (b) energy yieldTable 3. Comparative results of tracking methods at  $G=400$  W/m<sup>2</sup> and  $T=25$  °C

Tracking Method	Rising Time (s)	Energy Yield (Wh)
P&O (at $\Delta V=0.5$ V)	5.3	0.4299
P&O (at $\Delta V=3.5$ V)	0.8	0.4515
Asymmetrical FLC	4.4	0.4386
Optimized FLC by chimp algorithm	2	0.4581

Table 4. Fitness function values of tracking methods

Tracking Method	Fitness
P&O (at $\Delta V=0.5$ V)	0.9468
P&O (at $\Delta V=3.5$ V)	0.9558
Asymmetrical FLC	0.9704
Optimized FLC by chimp algorithm	0.9802

## 6. CONCLUSION

In this paper, an asymmetrical fuzzy MPPT method of seven triangular MFs is used. Where, its setting values are derived under STC. Furthermore, the fuzzy MPPT method is optimized by using the chimp algorithm taken into consideration different operating conditions included in the chosen fitness function. It is demonstrated from the simulation results in section 5, the asymmetrical FLC method cannot satisfy the optimal tracking performances at all test operating conditions. Nevertheless, its tracking effectiveness is conspicuous at STC. In contrast, the optimized tracking method by chimp algorithm can successfully investigate the optimal tracking performances at all test conditions. Moreover, it is evident that the optimized method has a largest fitness of 0.9802 compared with asymmetrical, P&O (at  $\Delta V=3.5$  V), and P&O (at  $\Delta V=0.5$  V) methods of 0.9704, 0.9558, and 0.9468 fitness values, respectively. Hence, it can be concluded that the optimized tracking method can successfully enhance the transient and steady state tracking performances for the PV systems. As future work, a fuzzy type-2 and another intelligent hybrid MPPT algorithms have to be explored and examined to conclude the best tracking algorithm for improving the overall PV performances.

## ACKNOWLEDGEMENTS




The authors would like to thank Mustansiriyah University ([www.uomustansiriyah.edu.iq](http://www.uomustansiriyah.edu.iq)), Baghdad-Iraq for its support in the present work.






## REFERENCES

- [1] Y. Li, Z. Tang, Z. Zhu, and Y. Yang, "A novel MPPT circuit with 99.1% tracking accuracy for energy harvesting," *Analog Integrated Circuits and Signal Processing*, vol. 94, no. 1, pp. 105–115, Jan. 2018, doi: 10.1007/s10470-017-1079-z.
- [2] M. Moutchou and A. Jbari, "Fast photovoltaic IncCond-MPPT and backstepping control, using DC-DC boost converter," *International Journal of Electrical and Computer Engineering (IJECE)*, vol. 10, no. 1, pp. 1101–1112, Feb. 2020, doi: 10.11591/ijece.v10i1.pp1101-1112.
- [3] A. Dandoussou, M. Kamta, L. Bitjoka, P. Wira, and A. Kuitché, "Comparative study of the reliability of MPPT algorithms for the crystalline silicon photovoltaic modules in variable weather conditions," *Journal of Electrical Systems and Information Technology*, vol. 4, no. 1, pp. 213–224, May 2017, doi: 10.1016/j.jesit.2016.08.008.
- [4] S. Zouirech, M. Zerouali, H. Elaissauoui, A. El Ougli, and B. Tidhaf, "Application of various classical and intelligent MPPT tracking techniques for the production of energy through a photovoltaic system," in *2019 7th International Renewable and Sustainable Energy Conference (IRSEC)*, Nov. 2019, pp. 1–6, doi: 10.1109/IRSEC48032.2019.9078154.
- [5] A. S. Samosir, H. Gusmedi, S. Purwiyanti, and E. Komalasari, "Modeling and simulation of fuzzy logic based maximum power point tracking (MPPT) for PV application," *International Journal of Electrical and Computer Engineering (IJECE)*, vol. 8, no. 3, pp. 1315–1323, Jun. 2018, doi: 10.11591/ijece.v8i3.pp1315-1323.
- [6] A. Heblib, T. Allaoui, A. Chaker, B. Belabbas, and M. Denai, "A comparative study of classical and advanced MPPT control algorithms for photovoltaic systems," *Przeglad Elektrotechniczny*, 2020, doi: 10.15199/48.2020.11.14.
- [7] A. Al-Gizi, M. Louzazni, M. A. Fadel, and A. Craciunescu, "Critical constant illumination time in comparison of two maximum power point tracking photovoltaic algorithms," *U.P.B. Sci. Bull., Series C*, vol. 80, no. 2, pp. 201–216, 2018.
- [8] Ö. F. Tozlu and H. Çalık, "A review and classification of most used MPPT algorithms for photovoltaic systems," *Hittite Journal of Science & Engineering*, vol. 8, no. 3, pp. 207–220, Sep. 2021, doi: 10.17350/HJSE19030000231.
- [9] W. I. Hameed, A. L. Saleh, B. A. Sawadi, Y. I. A. Al-Yasir, and R. A. Abd-Alhameed, "Maximum power point tracking for photovoltaic system by using fuzzy neural network," *Inventions*, vol. 4, no. 3, pp. 33–45, 2019, doi: 10.3390/inventions4030033.
- [10] R. B. Bollipo, S. Mikkili, and P. K. Bonthagorla, "Critical review on PV MPPT techniques: classical, intelligent and optimisation," *IET Renewable Power Generation*, vol. 14, no. 9, pp. 1433–1452, Jul. 2020, doi: 10.1049/iet-rpg.2019.1163.
- [11] A. Al-Gizi, S. AL-Chlaihawi, M. Louzazni, and A. Craciunescu, "Genetically optimization of an asymmetrical fuzzy logic based photovoltaic maximum power point tracking controller," *Advances in Electrical and Computer Engineering*, vol. 17, no. 4, pp. 69–76, 2017, doi: 10.4316/AECE.2017.04009.
- [12] S. Figueiredo and R. N. A. L. e S. Aquino, "Hybrid MPPT technique PSO-P&O applied to photovoltaic systems under uniform and partial shading conditions," *IEEE Latin America Transactions*, vol. 19, no. 10, pp. 1610–1617, Oct. 2021, doi: 10.1109/TLA.2021.9477222.
- [13] A. G. Abdullah, M. sh. Aziz, and B. A. Hamad, "Comparison between neural network and P&O method in optimizing MPPT control for photovoltaic cell," *International Journal of Electrical and Computer Engineering (IJECE)*, vol. 10, no. 5, pp. 5083–5092, Oct. 2020, doi: 10.11591/ijece.v10i5.pp5083-5092.
- [14] A. G. Al-Gizi, A. Craciunescu, and S. J. Al-Chlaihawi, "The use of ANN to supervise the PV MPPT based on FLC," in *2017 10th International Symposium on Advanced Topics in Electrical Engineering*, 2017, pp. 703–708, doi: 10.1109/ATEE.2017.7905128.
- [15] S. S. Mohammed, D. Devaraj, and T. P. I. Ahamed, "GA-optimized fuzzy-based MPPT technique for abruptly varying environmental conditions," *Journal of The Institution of Engineers (India): Series B*, vol. 102, no. 3, pp. 497–508, Jun. 2021, doi: 10.1007/s40031-021-00552-2.
- [16] P.-C. Cheng, B.-R. Peng, Y.-H. Liu, Y.-S. Cheng, and J.-W. Huang, "Optimization of a fuzzy-logic-control-based MPPT algorithm using the particle swarm optimization technique," *Energies*, vol. 8, no. 6, pp. 5338–5360, Jun. 2015, doi: 10.3390/en8065338.
- [17] A. H. Miry, A. H. Mary, and M. H. Miry, "Improving of maximum power point tracking for photovoltaic systems based on swarm optimization techniques," *IOP Conference Series: Materials Science and Engineering*, vol. 518, no. 4, 2019.
- [18] A. P. Yoganandini and G. S. Anitha, "A modified particle swarm optimization algorithm to enhance MPPT in the PV array," *International Journal of Electrical and Computer Engineering (IJECE)*, vol. 10, no. 5, pp. 5001–5008, Oct. 2020, doi: 10.11591/ijece.v10i5.pp5001-5008.
- [19] M. Slimi, A. Boucheta, and B. Bouchiba, "Maximum power control for photovoltaic system using intelligent strategies," *International Journal of Power Electronics and Drive Systems (IJPEDS)*, vol. 10, no. 1, pp. 423–432, Mar. 2019, doi: 10.11591/ijpeds.v10.i1.pp423-432.
- [20] E. Kandemir, N. S. Cetin, and S. Borekci, "A Comparison of perturb & observe and fuzzy-logic based MPPT methods for uniform environment conditions," *Periodicals of Engineering and Natural Sciences (PEN)*, vol. 5, no. 1, pp. 16–23, Mar. 2017, doi: 10.21533/pen.v5i1.67.
- [21] A. Al-Gizi, S. Al-Chlaihawi, and A. Craciunescu, "Efficiency of photovoltaic maximum power point tracking controller based on a fuzzy logic," *Advances in Science, Technology and Engineering Systems Journal*, vol. 2, no. 3, pp. 1245–1251, Jul. 2017, doi: 10.25046/aj0203157.
- [22] M. Lamnadi, M. Trihi, B. Bossoufi, and A. Boulezhar, "Comparative study of IC, P&O and FLC method of MPPT algorithm for grid connected PV module," *Journal of Theoretical and Applied Information Technology*, vol. 89, no. 1, pp. 242–253, 2016.
- [23] I. Yadav, S. K. Maurya, and G. K. Gupta, "A Literature review on industrially accepted MPPT techniques for solar PV system," *International Journal of Electrical and Computer Engineering (IJECE)*, vol. 10, no. 2, pp. 2117–2127, Apr. 2020, doi: 10.11591/ijece.v10i2.pp2117-2127.
- [24] M. Khishe and M. R. Mosavi, "Chimp optimization algorithm," *Expert Systems with Applications*, vol. 149, pp. 1–26, Jul. 2020, doi: 10.1016/j.eswa.2020.113338.
- [25] M. H. Zafar, N. M. Khan, A. F. Mirza, and M. Mansoor, "Bio-inspired optimization algorithms based maximum power point tracking technique for photovoltaic systems under partial shading and complex partial shading conditions," *Journal of Cleaner Production*, vol. 309, Aug. 2021, doi: 10.1016/j.jclepro.2021.127279.
- [26] S. Krishnan and K. Sathiyasekar, "A novel salp swarm optimization MPP tracking algorithm for the solar photovoltaic systems under partial shading conditions," *Journal of Circuits, Systems and Computers*, vol. 29, no. 01, Jan. 2020, doi: 10.1142/S0218126620500176.
- [27] A. F. Mirza, M. Mansoor, Q. Ling, B. Yin, and M. Y. Javed, "A salp-swarm optimization based MPPT technique for harvesting maximum energy from PV systems under partial shading conditions," *Energy Conversion and Management*, vol. 209, Apr. 2020, doi: 10.1016/j.enconman.2020.112625.




**BIOGRAPHIES OF AUTHORS**

**Ammar Al-Gizi**    was born in Baghdad, Iraq, in 1978. He received the B.Sc. degree in electrical engineering and the M.Sc. degree in electronic and communication engineering from Al-Mustansiriyah University, Baghdad, Iraq, in 1999 and 2003, respectively. He received the Ph.D. degree from the Faculty of Electrical Engineering, University “POLITEHNICA” of Bucharest (UPB), Romania. He is currently an Asst. Prof. in Electrical Engineering Department, Mustansiriyah University, Iraq. His current research interests include the use of intelligent control and evolutionary algorithms in the renewable and sustainable energy systems. He can be contacted at email: ammar.ghalib@uomustansiriyah.edu.iq.



**Abbas Hussien Miry**    received his B.Sc. degree in Electrical Engineering in 2005 from the Mustansiriyah University and his M.Sc. degree in control and computer engineering in 2007 from Baghdad University. He received a Ph.D. degree in 2011 in control and computer engineering from the Basrah University, Iraq. In 2007. His recent research activities are artificial intelligence, control and swarm optimizations. He can be contacted at email: abbasmiry83@uomustansiriyah.edu.iq.



**Mohanad Abd Shehab**    received the B.Sc. and M.Sc. degrees in Electrical and Electronic Engineering, from the University of Technology, Iraq, in 1996 and 1998 respectively, and Ph.D. degree in Electronic Engineering, from Yildiz Technical University, Turkey, in 2018. He is currently a lecturer in the Electrical Engineering department, Mustansiriyah University, Iraq. His research interests include image and signal processing, ANN, pattern recognition, and machine learning. He can be contacted at email: mohanadshehab@uomustansiriyah.edu.iq.